Materials and Manufacturing Processes, 30: 41–46, 2015

ISSN: 1042-6914 print/1532-2475 online
DOI: 10.1080/10426914.2014.930955

Taylor & Francis
Taylor & Francis Group

Experimental and Theoretical Investigation of Powder–Binder Mixing Mechanism for Metal Injection Molding

Altab Hossain, Imtiaz Ahmed Choudhury, Nurun Nahar, Ismail Hossain, and Azuddin Bin Mamat

Department of Mechanical Engineering, Faculty of Engineering, University of Malaya, Kuala Lumpur, Malaysia

Metallic powder and binder mixing mechanism plays a vital role in the quality of molded parts in metal injection molding. The present study is intended for experimental and theoretical investigation of powder–binder mixing mechanism to investigate the functional correlation among mixing parameters and performance characteristics for different composition of feedstocks. Powder loading and shear rate are considered as input parameter. Fuzzy expert system is adopted to test the validity of the experimental results by analyzing different numerical error criteria using the viscosity as output with respect to input parameters. The mean relative error and correlation coefficient for type ***A*** and type ***B*** were found to be 6.09% and 8.51% (<10%) and 0.990 and 0.998, respectively. Hence the result indicates a reliable acceptability of the proposed amount of powder loading for feedstock preparation.

Keywords Binder; Debinding; FES; Injection; Mixing; Powder; Rheology; Shear; Sintering; Viscosity.

Introduction

Metal injection molding (MIM) is a manufacturing technique where finely divided powdered metal is mixed with a measured amount of binder to compose feedstock which is processed through injection mold forming to produce precision and parts of complicated shape at low cost. MIM has four main processing stages such as (i) mixing, (ii) injection molding, (iii) debinding, and (iv) sintering [1].

In powder injection molding as well as in ceramic injection molding, lower percentage of powder loading results in complete mold filling and improved green strength while it causes shrinkage during debinding and sintering [2–4]. Shrinkage during sintering causes poor dimensional control in the brown (sintered) part [5]. On the contrary, higher percentage of powder causes insufficient amount of binder which cannot fill the die cavity entirely [6]. Therefore, an optimal mixing mechanism with ideal powder and binder composition ratio is vital. The typical powder–binder ratio in the feedstock is about 60:40 by volume whereas aluminum mixture constitutes about 86% powder by weight for typical mix ratio [7, 8]. Feedstock performance and product quality is subjected to the important properties and process parameters such as viscosity, density, mixing speed, melting range, barrel temperature, mold temperature, and powder loading [9–11]. These mixing parameters and performance characteristics perform non-linearly and interact, thus making it very difficult to create an exact mathematical model.

In metal injection area, a number of researches have been carried out with 316 L stainless steel fine powders and different binders [4]. However, very few investigations have been carried out on the effects of composition ratio between aluminum powder and binder system. Again in the past, a large number of models such as response surface methodology, artificial neural network (ANN) models, and Taguchi method have been used to evaluate the performance characteristics and process parameters [10–13]. Moreover, ANN model requires large amounts of noise free experimental data for parameters optimization, which are time-consuming process. Conversely, fuzzy logic expert system (FLES) uses expert's appraisal as well as a logical system closer to human knowledge. Because of this reason, fuzzy expert system (FES) is used in the present study to observe the perfection of feedstock by viscosity analysis [14].

In the present investigation, pure alumina powders have been enumerated to fashion the feedstock due to its good mechanical properties and excellent thermal conductivity. FES is used to investigate powder–binder mixing mechanism for MIM due to its expert logical system. The study consists of experimental and theoretical analysis.

Materials and Methods

Mixing experiments were conducted in a Retsch planetary ball mill PM 100. The microstructure of the aluminum powder particles was observed using the scanning electron microscopy (SEM) (JEOL JSM-7600F). With the composition of powder and binder (Table 1), four feedstocks have been prepared at 350 rpm mixing speed and mixing time of 6 h and viscosity was measured

Received March 19, 2014; Accepted May 7, 2014

Address correspondence to Altab Hossain, Department of Mechanical Engineering, Faculty of Engineering, University of Malaya, Kuala Lumpur 50603, Malaysia; E-mail: altab75@um.edu.my

Color versions of one or more of the figures in the article can be found online at www.tandfonline.com/lmmp.

TABLE 1.—Identification for various powder and binder composition.

Binder	Powder loading (wt%)	HDPE (wt%)	PW (wt%)	SA (wt%)	Label
Type *A*	58.0	23.10	14.70	4.20	*A*58
	62.0	20.90	13.30	3.80	*A*62
Type *B*	58.0	35.00	—	7.00	*B*58
	62.0	32.00	—	6.00	*B*62

using a Physica MCR 301 Rheometer (Alpha Analytical, 80945628). Each feedstock was loaded onto the pre-heated barrel at 90°C. Viscosity of the usable mixture is required to be less than 1000 Pa s for shearing rate range of 100–1000 s^{-1}. In the subsequent stages, the green injection molded part was debinded and sintered to get the final product. All the experiments were conducted in the laboratory of University of Malaya.

Aluminum powder of 99.9% purity, with particle size of range 0–60 μm and relative density of 2.7 g/cm^3, was used in the feedstock preparation. The used aluminum powders were of small grain size and regular shape which has a tendency to agglomerate. Similar to the earlier articles on MIM, binder system consisting of paraffin wax (PW), stearic acid (SA), and high density polyethylene (HDPE) was chosen according to the inter-relations and suitability toward the metal powder used [1, 2, 15]. Two types of multi-component binder systems were prepared for analysis and testing. In type *A*, 55 wt% HDPE, 35 wt% PW, and 10 wt% SA were mixed together; while in type *B*, 83 wt% HDPE and 17 wt% SA were mixed as shown in Table 1 [1].

Pseudo-plastic fluid which exhibits shear-thinning properties is correlated by an empirical mathematical equation named Power Law as follows [16]:

$$\tau = K(\dot{\gamma})^n \tag{1}$$

where τ is for shearing stress (Pa), $\dot{\gamma}$ is the shearing rate (s^{-1}), K is fluid consistency coefficient (dimensions depend on the numerical value of n), and n is flow exponent (<1). Shearing susceptibility is higher for low flow exponent [1]. Further, material becomes dilatant and powder and binder would separate under high shear rate at $n > 1$ [16]. Feedstock's viscosity decreases as shearing rate increases. Too high viscosity of feedstock sometimes causes difficulties in mold filling as well as failure during injection molding [1]. However, low viscosity of feedstock is prospective for injection molding. The significant rheological characteristic viscosity, η, of feedstock can be defined by the following relation [16]:

$$\eta = \frac{\tau}{\dot{\gamma}} \tag{2}$$

By combining Eqs. (1) and (3), the general shear rate-dependence of viscosity can be defined by using the following equation [16]:

$$\eta = K(\dot{\gamma})^{n-1} \tag{3}$$

FIGURE 1.—Custom-made vertical metal injection molding machine.

The injection of feedstock to the mold was carried out using a custom-made injection molding machine (Fig. 1) at 7 bar injection pressure and 80–100°C injection temperatures. Green parts of different geometrical shapes including the tensile (of dimension 64 mm × 10 mm × 3 mm) and various gear sizes were produced as shown in Fig. 2. Solvent debinding of the green part was done by immersing the specimen in hexane and heating was conducted at 50°C for 5 h. The solvent debond parts were dried using dry air blower at a temperature of 50°C. The solvent contaminated with the binder after debinding was distilled and recycled. Significant volume shrinkage and weight reduction was observed at the end of solvent debinding due to the elimination of PW and SA confirmed through SEM analysis and weight measurement before and after solvent debinding. Subsequently, the green part was debinded thermally in a vacuum furnace at 250–500°C for 30–90 min. Few of all debond components exhibited

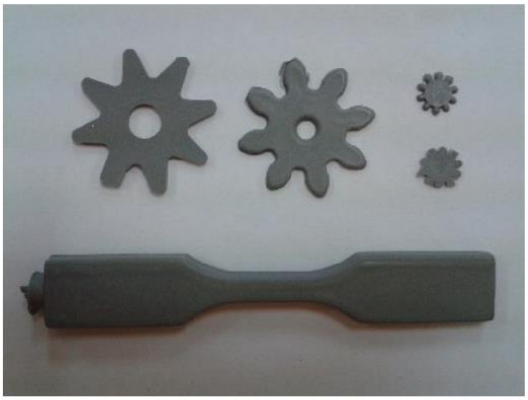

FIGURE 2.—Various shapes of green parts produced by injection molding process.

certain degrees of inclination and bending during debinding stage due to the inhomogeneity found in some areas of specimen. The parts were sintered under vacuum phase at 580–640°C for 30–120 min according to the sintering cycle designed by Nyborg et al. [17]. The effects of temperature on the sintered parts were monitored which is necessary for better dimensional control as mentioned by Onbattuvelli et al. [18].

The use of FLES has been proposed as a diagnostic formula [19] to determine the viscosity of feedstock, shear rate, and powder loading using the results of experimental analysis. In this study, a fuzzy expert model has been developed and used to investigate the optimal mixing conditions of MIM as a decision-making support tool.

The input variable shear rate (SR) was given eight possible lingual transistorizes, namely, very low (VL), low (L), low medium (LM), medium (M), high medium (HM), medium high (MH), high (H), and very high (VH); while five lingual transistorizes, namely, low (L), medium (M), medium high (MH), high (H), and very high (VH) were used for input variable powder loading (PL). Twelve output fuzzy sets (level 1–12) were considered for viscosity (VT). A total of 40 fuzzy rules (Table 2) were formed based on expert knowledge and past experience.

There is a level of membership for each lingual word that applies to that input variable. Fuzzifications of the factors were made by using following relations:

$$SR(i_1) = \begin{Bmatrix} i_1; & 100 \le i_1 \le 1000 \\ 0; & \text{otherwise} \end{Bmatrix} \quad (4)$$

$$PL(i_2) = \begin{Bmatrix} i_2; & 58 \le i_2 \le 62 \\ 0; & \text{otherwise} \end{Bmatrix} \quad (5)$$

$$VT(o_1) = \begin{Bmatrix} o_1; & 1 \le o_1 \le 73.8 \\ 0; & \text{otherwise} \end{Bmatrix} \quad (6)$$

$$VT(o_2) = \begin{Bmatrix} o_2; & 14 \le o_2 \le 332 \\ 0; & \text{otherwise} \end{Bmatrix} \quad (7)$$

TABLE 2.—Fuzzy inference rules.

	Input variables		Output variables (VT)	
Rules	SR	PL	Type *A*	Type *B*
1	VL	L	L9	L9
—	—	—	—	—
7	H	L	L2	L2
—	—	—	—	—
14	MH	M	L3	L3
—	—	—	—	—
24	VH	MH	L1	L1
—	—	—	—	—
33	VL	VH	L12	L12
—	—	—	—	—
40	VH	VH	L1	L1

where i_1 and i_2 are the first and second input variable *SR* and *PL* and o_1 and o_2 are the first and second output variables viscosity, respectively. The membership functions for all input and output variables are developed using fuzzy toolbox in MATLAB. In defuzzification stage, final output fuzzy set are defuzzified using the following equation:

$$VT^{crisp} = \frac{\sum_i b_i \mu_{(i)}}{\sum_i \mu_{(i)}} \quad (8)$$

where b_i is the position of the singlet in the ith universe, and $\mu_{(i)}$ is the firing strength of actual terms of rule i. Using Eq. (8), the crisp value of viscosity, VT, was obtained as 27.9 and 44 Pa s for type *A* and type *B*, respectively.

RESULTS AND DISCUSSION

After completing the rheological testing, the data of the shear stress for each feedstock formulation was obtained by measuring the pressure drop across the die. For all feedstocks log τ–log $\dot{\gamma}$ graphs have been plotted as shown in Fig. 3. Throughout the experiment, viscosity decreases with the increase in shearing rate and increases with increasing powder volume fraction. Similar results using binder components were reported in the past for alumina powder by Thomas-Vielma et al. [1] and Si_3N_4 by Lenz et al. [20]. However, the flow behavior index or flow exponent values were different.

From Fig. 3, the values of flow behavior index can be obtained as $n_{A58} = 0.0796$ and $n_{A62} = 0.0801$ for type *A* and $n_{B58} = 0.106$ and $n_{B62} = 0.108$ for type *B*. It is also noticed that the flow behavior index of the feedstock has started to increase as powder loading increases from 58% to 62% for both binder systems, achieving the lowest value of 0.0796 and 0.0801 for type *A* with the feedstock of 58% and 62% powder loading, respectively. Figure 4 shows the rheological characteristics of the feedstock formulations under various conditions for type *A* and type *B*.

It is observed that the viscosity for both type *A* and type *B* decreases approximately at a rate of 10% with

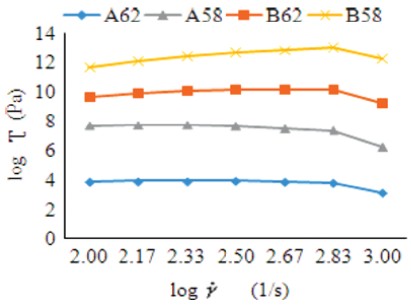

FIGURE 3.—Relations of shear stress and shear rate for feedstocks.

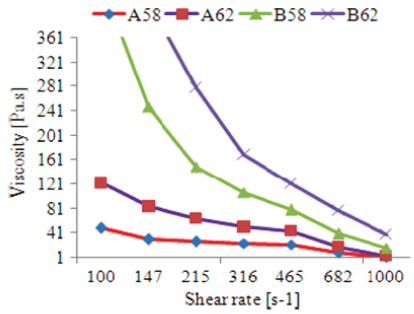

FIGURE 4.—Effects of shear rate and powder loading on viscosity (Type *A* and Type *B*).

increasing 47% of shear rate between the range of 147–465 and 465–682 s^{-1}, respectively. However, viscosity tremendously decreases by 58–86% (for type *A*) and 40% (for type *B*) with the increase of 47% shear rate within 465–1000 and 682–1000 s^{-1}, respectively. In contrast, viscosity increases slowly approximately 3–14% at shear rate 316, 465, 682, and 1000 s^{-1} (type *A*) and 0.60–7% at shear rate 100, 147, and 316 s^{-1} (type *B*) with the increase of 7% powder loading. In addition, viscosity increases significantly about 40–80% with the same increasing of powder loading at shear rate 100, 147, and 215 s^{-1} for type *A* while it increases enormously approximately 50–86% at shear rate 215, 465, and 682–1000 s^{-1} for type *B*. Practically, it is observed that the viscosity reaches the peak 73.8 Pa s (type *A*) and 332 Pa s (type *B*) when the powder loading reaches its maximum level of 62%.

In this experimental investigation, flow behavior index and peak value of viscosity was observed to be lowest for type *A*. Though flow exponent value was smaller for 58% powder loading, smaller peak value of viscosity was observed for 62% powder loading. Considering the condition for viscosity, shear rate, and powder volume loading in MIM process, it can be concluded that type *A* with 62% powder loading is the most appropriate compared to type *B*. The present experimental result is found to be in good agreement with the findings of Thomas-Vielma et al. [1] and Kong et al. [4] where the previous researcher's best powder loading was in between 58% and 66%.

The final output viscosity of the fuzzy logic system is verified by changing the input variable values in the MATLAB® rule viewer. Using MATLAB, the fuzzy control surfaces were developed as shown in Fig. 5(a) and 5(b). In the present study, SR of 100–1000 s^{-1} and PL of 58–62% were used as input and VT between 1–74 and 14–332 Pa s were used as output for type *A* and type *B*, respectively, for fuzzy model development. After developing the model, the viscosity was predicted from rule viewer. The fuzzy prediction model with input variable SR 100 s^{-1} and PL 62% was used and out variable viscosity was obtained as 71.9 Pa s while the experimental value was 73.8 Pa s. Decisively, it can be concluded that the developed fuzzy model can help in the selection of significant mixing parameters and their required level in MIM process to achieve a targeted level of product quality.

The results of the theoretical investigation through FLES were compared with the experimental results. The correlations between measured values and predicted values of viscosity in different mixing and process conditions have been demonstrated in Fig. 6. The correlation coefficient (R) from the actual and predicted values of viscosity found to be 0.990 ($R^2 = 0.981$) for type *A* and 0.998 ($R^2 = 0.996$) for type *B* showed that developed fuzzy models might explain up to 98.1% and 99.6% (for type *A* and *B*, respectively) of the total variability of viscosity. The mean relative errors were obtained as 6.09% and 8.51% for type *A* and type *B*, which were less than 10% for both cases. The goodness of fit values was found to be 0.990 and 0.998 for type *A* and type *B*, respectively, which were close to 1.0. All the results of the correlation coefficient, the mean relative error, and the goodness of fit are showing very powerful ability and accuracy of the developed model.

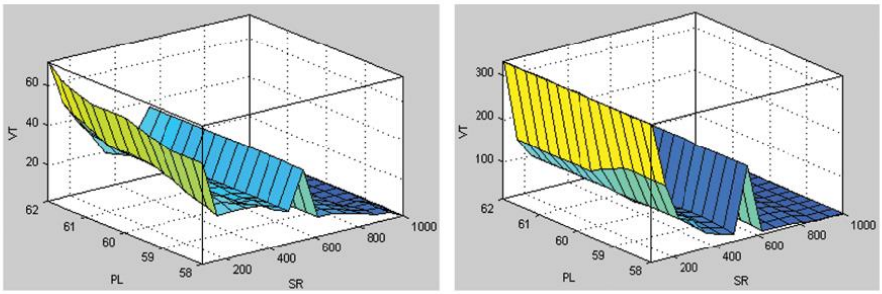

(a) Type *A* (b) Type *B*

FIGURE 5.—Control surfaces of fuzzy inference system.

Link to Full-Text Articles :

http://www.tandfonline.com/doi/abs/10.1080/10426914.2014.930955#.VRIhCo7fV5k

http://www.ingentaconnect.com/content/tandf/amp/2015/00000030/00000001/art00004